J Mater Sci: Mater Med (2008) 19:3561–3566
DOI 10.1007/s10856-008-3520-4

Effect of filler size and shape on local nanoindentation modulus of resin-composites

Konstantinos Masouras · Riaz Akhtar · David C. Watts · Nick Silikas

Received: 20 March 2008 / Accepted: 19 June 2008 / Published online: 15 July 2008

Abstract The aim of this study was to determine the Young's moduli (E) of a series of model dental resin-composites using nanoindentation, and to examine how E was influenced by differences in filler-size and shape. Materials with different filler-sizes and shapes but constant filler volume-fraction were investigated. Disc specimens, mounted in polystyrene resin were mechanically polished and tested with a nanoindenter. One-way ANOVA and Bonferroni test were used for the statistical analysis. Regression analysis was used to investigate the correlation between E and filler-size. E ranged from 9.31 to 12.54 GPa for spherical fillers and from 14.09 to 17.03 GPa for irregular fillers. Statistically significant differences were found among the groups. Strong quadratic correlations were observed between E and filler-size for unimodal materials with spherical and irregular fillers, but were not statistically significant. Filler-size and shape seemed to be fine-tuning factors for E.

1 Introduction

The quest for new materials of improved performance drives the re-design of dental resin-composites, especially as regards filler-size reduction. It is expected that the incorporation of smaller-sized particles in the resin-matrix will enhance aesthetic characteristics and mechanical strength.

Several resin-composites are now available containing filler particles ranging from a few nm (10 nm) to a few microns (2–3 μm) [1]. Smaller filler sizes contribute towards good surface polishing and consequently high gloss, as found with the homogeneous micro-filled (0.04 μm) resin-composites. Size reduction allows for closer particle packing, thus resin-composites with very high filler volume fraction can be fabricated, resulting in good aesthetic properties without compromising their mechanical and wear characteristics.

A key mechanical property of dental resin-composites is their stiffness or Young's modulus. In the last few years, nanoindentation has been used to determine the Young's modulus of dental materials, such as ceramics [2], dental resins [3] and dental resin-composites [4, 5]. The technique has been used to study the effect of different fillers on the mechanical properties of dental composites [4]. However, there is little quantitative information in the literature on the relationship between filler size or shape and Young's modulus.

The aim of this study was to determine the Young's modulus for a series of model resin-composites using nanoindentation and to investigate the effect of filler size and shape on the moduli. The null hypotheses were that filler size and shape would not affect Young's moduli.

2 Materials and methods

Twelve model resin-composites (Ivoclar Vivadent, Schaan, Liechtenstein) were tested in this study (Table 1). All materials had the same resin matrix and constant filler

K. Masouras · D. C. Watts · N. Silikas (✉)
Biomaterials Science Research Group, School of Dentistry, The University of Manchester, Higher Cambridge Street, Manchester M15 6FH, UK
e-mail: nick.silikas@manchester.ac.uk

R. Akhtar
School of Materials, The University of Manchester, Grosvenor Street, Manchester M1 7HS, UK

D. C. Watts
Photon Science Institute, The University of Manchester, Oxford Road, Manchester M13 9PL, UK

Table 1 Material composition

Material code and shape[a]	Mean filler size (nm)		Wt.%
Spherical fillers			
I-S	Unimodal	100	72.3
II-S		250	72.6
III-S		500	
IV-S		1000	72.5
V-S	Multimodal	100:250:1000 (1:1:2)	72.0
VI-S		100:1000 (1:3)	
Irregular fillers			
VII-G	Unimodal	450	76.4
VIII-G		700	
IX-G		1000	
X-G		1500	
XI-G	Multimodal	450:1000 (1:3)	
XII-G		450:700:1500 (1:1:3)	

The resin matrix consisted of Bis-GMA, UDMA, TEGDMA and the filler volume fraction was constant at 56.7%, for all materials

[a]S series: Spherical (SiO_2); G series: Irregular (Ba–Al–B-silicate glass)

volume-fraction (56.7 vol.%) but various filler shapes, sizes and size distribution. Half of the samples had spherical fillers of 100–1000 nm and the other half had irregular fillers of 450–1500 nm. The spherical fillers were SiO_2 and have a modulus of 72.1 GPa [6]. Although there is no reported modulus values for the Ba–Al–B-silicate glass irregular fillers in literature, a similar composition of Ba–Al–B–Ca–Mg-silicate glass has a value of 89.1 GPa [7].

Disc specimens (12 mm × 2 mm) were prepared from each material by injecting the resin-composite into a Teflon mould. Two microscopic glass slides, covered with transparent polystyrene matrix strips, were used to compress the material in the mould. The samples were irradiated for 40 s from each surface with a halogen light curing unit (Elipar Trilight, 3M-ESPE, Seefeld, Germany) operated in standard mode and of 550 mW/cm^2 irradiance, as measured with the calibrated radiometer incorporated. After polymerization, the specimens were mounted in a 2.5 cm diameter phenolic ring forms (Buehler, Coventry, UK) and embedded in self-curing polystyrene resin (Castoglas Resin, Buehler, Coventry, UK).

The embedded specimens were next submitted to mechanical finishing in a grinding machine rotating with 200 rpm (Saphir 330, Mager Scientific Inc., Dexter, MI, USA), with a sequence of SiC papers of decreasing abrasiveness (320-, 400-, 600-, 800- and 1200-grit) under continuous water cooling. The specimens were further polished in a polishing machine (Buehler, Coventry, UK) by using a sequence of felt cloths (Whitefelt, Buehler, Coventry, UK) with 3, 1 and 0.25 μm embedded diamond, Al_2O_3 and SiO_2 grains under periodical lubrication with an oil based lubricant (Metadi, Buehler, Coventry, UK). Each step was carried out for 120 s. Finally, the specimens were sonicated in an ultrasonic water bath (Elma transsonic T 310, Shalltec, Singen, Germany) for 5 min to remove any remaining debris.

Nanoindentation measurements were performed using an MTS XP nanoindenter (MTS Systems Co., Nano Instruments, Oak Ridge, TN, USA) equipped with a Berkovich (three-sided pyramidal) diamond tip (100 nm radius). The load and displacement resolution of the instrument were 50 nN and 0.01 nm respectively. The continuous stiffness measurement (CSM) technique [8] was used to determine the stiffness of the samples continuously as a function of depth. Calibration indents were made on fused silica.

Thirty indentations on randomly selected areas were performed on each resin-composite sample. The indents were located at least 20 μm apart to avoid the influence of residual stresses from adjacent impressions. Testing was undertaken at room temperature and began once thermal drift had stabilized below 0.05 nm/s.

Each testing cycle consisted of four segments (Fig. 1): the loading segment; the peak load holding segment; the unloading segment; and the holding segment at 10% of maximum load after which the specimen was fully unloaded. The initial contact of the indenter with the surface was identified by the change in stiffness. The data used for the

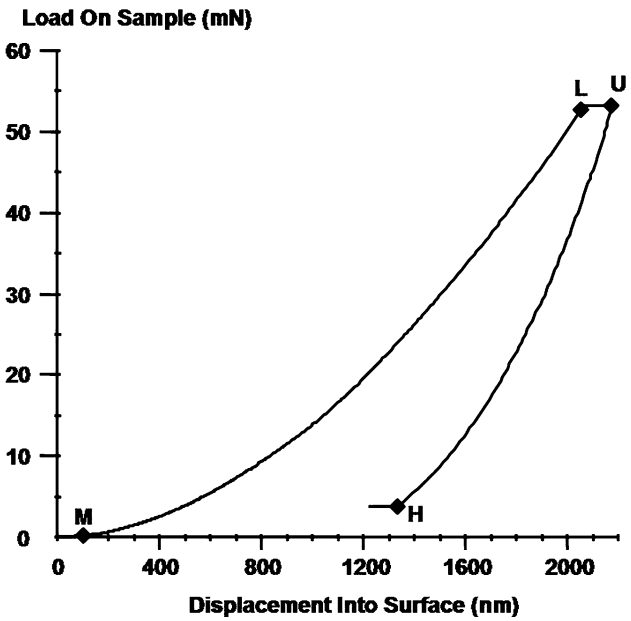

Fig. 1 Typical load–displacement graph of a nanoindentation. M: Index for the first data point included in the calculation of average hardness and modulus. L: Index for the last data point in the loading segment. U: Index for the data point corresponding to the start of unloading. H: Index for the data point corresponding to the start of the hold for thermal drift

calculation of the elastic modulus were those obtained over a depth range from 100 to 2000 nm. Data collection and analysis were conducted using the software provided by MTS (Test Works 4, MTS Systems Co., Nano Instruments, Oak Ridge, TN, USA). The modulus obtained from analysis of the raw data (load–displacement curve, Fig. 1) incorporates stiffness of the sample and the indenter. This is usually referred to as the "reduced or combined" modulus [9, 10]. The relationship of the reduced modulus to the Young's modulus of the material is given by Eq. 1.

$$\frac{1}{E^*} = \frac{1-\nu^2}{E} + \frac{1-\nu_{\text{ind}}^2}{E_{\text{ind}}} \quad (1)$$

where E^* is the reduced modulus, ν and E are the Poisson's ratio and Young's modulus respectively of the material and ν_{ind} and E_{ind} are the Poisson's ratio and Young's modulus respectively of the indenter. The Poisson's ratio values of both the indenter and the material, as well as the Young's modulus of the indenter must be known in order to determine the Young's modulus of the material.

The microstructure was characterised using scanning electron microscopy (SEM). Specimens, were mounted on aluminum stubs, sputter-coated with carbon and observed under a Field-Emission Gun Scanning Electron Microscope (FEG-SEM Philips XL 30, Eindhoven, The Netherlands) under 10 kV accelerating voltage. The spot size was 2 nm.

One way ANOVA and Bonferroni post-hoc multiple comparison test at a level of significance $P < 0.05$, were used for the statistical analysis. A regression and correlation analysis was performed to determine any possible correlation between Young's moduli and filler sizes.

3 Results

The mean Young's moduli of all resin-composites tested are presented in Table 2. In all cases, a Poisson's ratio of 0.3 for resin-composites was used in Eq. 1. Analysis of variance revealed statistically significant differences among the groups at $P < 0.05$.

All materials with spherically shaped fillers presented significantly lower moduli values than the ones with irregularly shaped fillers. The values for the former ranged between 9.31 GPa (I-S) and 12.54 GPa (V-S) while for the latter between 14.09 GPa (VII-G) and 17.03 GPa (X-G).

Most of the materials had a unimodal distribution of fillers. However, there were four resin-composites (V-S, VI-S, XI-G and XII-G) where a multimodal distribution of filler sizes existed. The correlation between Young's moduli and filler sizes for the unimodal materials is presented in Fig. 2. There was a trend towards an increase of modulus with increasing filler size for both types of fillers. Furthermore, both spherical filler and irregular filler materials presented a strong quadratic correlation between Young's moduli and filler sizes as confirmed by the high r values. For spherical filler materials P was 0.228 and r was 0.97, while for irregular filler materials P was 0.345 and r was 0.94. On the other hand, the P values indicated no statistically significant correlations. Young's moduli of multimodal materials (spherical and irregular filler shapes) are presented in Fig. 3. These were examined separately since estimation of the mean filler size of multimodal materials can be difficult and lead to incorrect placement of these materials on the filler size axis of the correlation graphs, and thus to imprecise correlation results.

Table 2 Mean Young's modulus and standard deviation in parenthesis of the resin-composites tested

Material	Young's modulus (SD) (GPa)
Spherical fillers	
I-S	9.31 (0.12) a
II-S	11.29 (0.21) b
III-S	12.08 (0.19) c
IV-S	12.17 (0.25) c
V-S	12.54 (0.33) c
VI-S	11.00 (0.26) b
Irregular fillers	
VII-G	14.09 (0.28) d
VIII-G	14.37 (0.25) d
IX-G	16.71 (0.35) f
X-G	17.03 (0.59) f
XI-G	15.73 (0.36) e
XII-G	15.69 (1.29) e

Poisson's ratio was assumed to be 0.3 for all materials. Groups with same small letter have no statistically significant difference between them

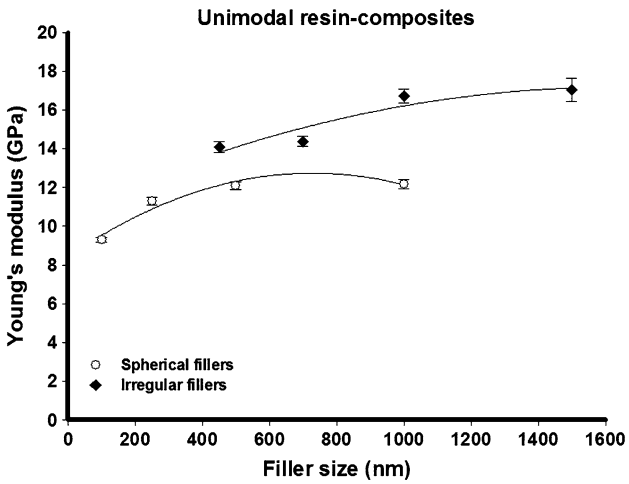

Fig. 2 Correlation of Young's moduli with filler sizes for unimodal materials with spherical and irregular fillers

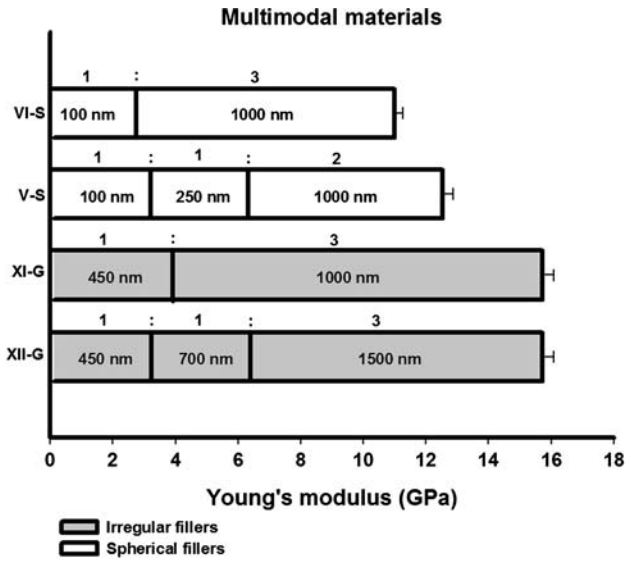

Fig. 3 Young's modulus of multimodal materials

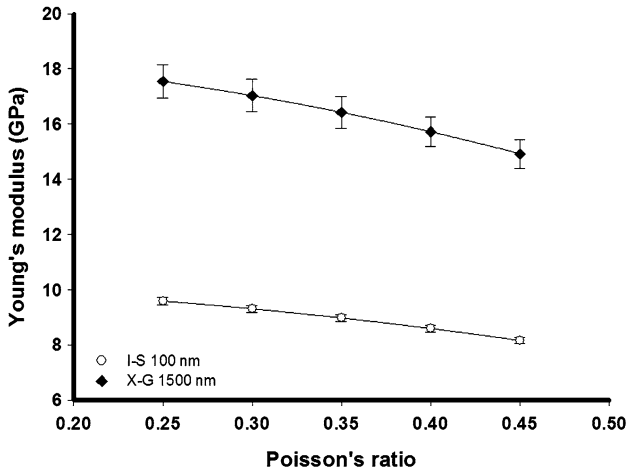

Fig. 4 Correlation of Young's modulus with Poisson's ratio for the materials with the highest and lowest modulus. Various Poisson's ratio values were assumed for the resin-composites

The Young's modulus calculated for the materials is dependent on the value of Poisson's ratio. This relationship was explored for two representative materials and presented in Fig. 4. The calculated Young's modulus decreases quadratically with increasing Poisson's ratio.

Representative SEM images are shown in Figs. 5 and 6.

4 Discussion

The materials used in this study had filler size ranging between 100 and 1500 nm. The use of the nanoindentation technique requires a very smooth and flat sample surface. If the amplitude of the surface asperities is large, the indenter will only have sporadic contact points with the material

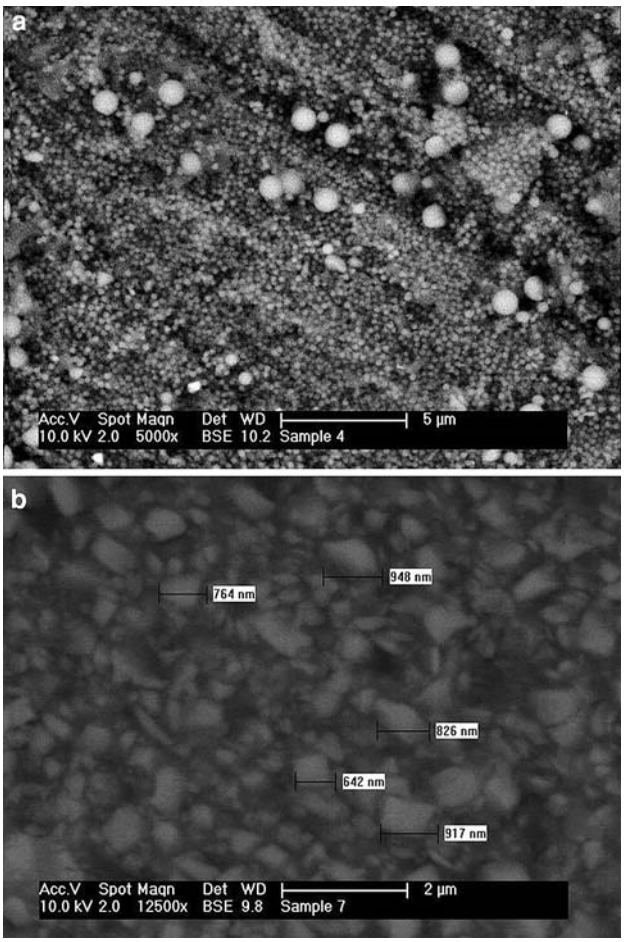

Fig. 5 (**a**) SEM image of *II-S* which contained spherical fillers with nominal size of 250 nm (×5000). Larger fillers were also detected. (**b**) SEM image of *VIII-G* which contained irregular fillers with nominal size of 700 nm (×12,500), where smaller and larger fillers could be observed

until it penetrates below the surface. The real contact area will be smaller than the one assumed by the depth measurement and indenter geometry, and consequently the apparent Young's modulus will be smaller [11].

Fused silica was chosen as calibration material because it is isotropic and has uniform properties on and below the surface and does not pile-up [8, 12].

The resin-composites tested had nominal mean filler size according to the manufacturer shown in Table 1. However, it is uncommon to encounter resin-composites with just one filler size. Most commercial formulations have a mixture of filler sizes with a mean value given by the manufacturer. This was evident in the present study too, as the SEM images revealed a variation in the filler sizes even for the nominally unimodal resin-composites (Fig. 5). Estimating a mean filler size of bimodal and multimodal materials (Fig. 6), was even more complicated. Therefore, these materials were excluded from the correlation figures as any

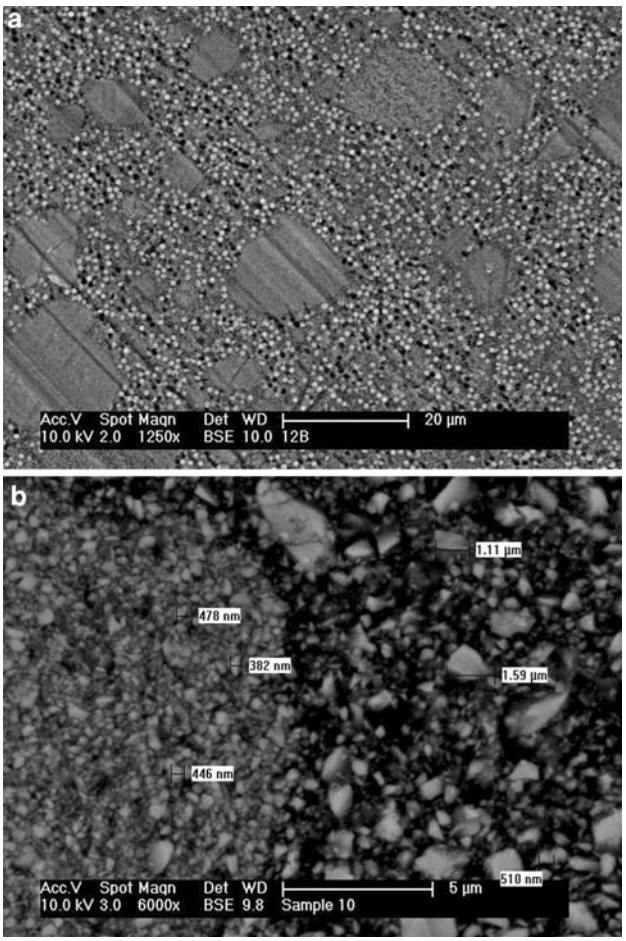

Fig. 6 (**a**) SEM image of *V-S* which contained a mixture of spherical fillers with nominal size of 100, 250 and 1000 at a ratio 1:1:2 (×1250). The discernible "patches" were small size filler agglomerations. (**b**) SEM image of *XI-G* in a higher magnification, which contained a mixture of irregular fillers with nominal size of 450 and 1000 nm at a ratio 1:3 (×6000). The boundary between an agglomeration, which consisted of 450 nm primary fillers (*left side*) and the dispersed fillers which were a mixture of 450 and 1000 nm (*right side*) is presented

deviation of the actual filler size from the one estimated, would lead to stronger or weaker correlations.

According to the results in Table 2, a tendency of increased Young's modulus as the filler size increased was observed. Thus, the null hypothesis was rejected. The correlation between Young's modulus and filler size was found to follow a quadratic pattern rather than a linear relationship. The high correlation coefficients for the unimodal materials (r: 0.97 for spherical and r: 0.94 for irregular) implied a relatively strong quadratic correlation. But the P values showed no statistically significant correlation. Additional points in each series would help elucidate the type of correlation further and provide more conclusive evidence, in case that the existing correlation is coincidental.

Despite the significant differences between materials, one could discern a more macroscopic grouping into three categories; one with filler size below 450 nm, a second one with filler size between 450 and 1000 nm and finally a third one with filler size above 1000 nm. This observation can be strengthened by the fact that for materials with only one size of spherical fillers, where direct comparisons are safer without additional confounding factors, the 500 nm and the 1000 nm groups did not have statistically significant differences. The same applies for the single-size irregular fillers, where the 1000 nm and the 1500 nm groups were not significantly different statistically.

Nanoindentation has been used for investigating local elasticity and hardness [13]. The small loads applied and the limited depths of penetration give little information about the bulk of the material. Thus, Young's modulus values must be examined in conjunction with the microstructure of the material's surface. In resin-composites, small fillers tend to aggregate in the resin matrix and form agglomerations whose dimensions can exceed 20 µm (Fig. 6). These formations are found dispersed among the rest of the fillers [1]. Due to the radius of the indenter tip (100 nm), an indentation can be started with the indenter touching only one filler or the interface of fillers and resin matrix. The deeper the indentation, the more representative the results of Young's modulus are for the composite material, as the increase of the indenter's projected area, with depth, ensures the inclusion in the measurement of a wider material area which contains both fillers and resin matrix.

An interesting observation derived from the results was that spherical filler materials had lower Young's modulus values than irregular filler materials irrespective of their filler size. This is probably due to the increased modulus of the irregularly shaped Ba–Al–B-silicate filler particles. Differences may be further attributed to the possibility of less hindered rearrangement of the spherical fillers thus reducing the stiffness of the composite. Irregular shape fillers may interlock more easily, thus not being able to rearrange their position and ultimately giving a mechanically stiffer material [14].

The assumption regarding the indenter's Young's modulus and Poisson's ratio, can affect the "real" value of the material's modulus. Similarly, an assumed Poisson's ratio affects the measurement. For dental resin-composites, Poisson's ratio values from less than 0.3 to more than 0.4 have been reported in the literature [15–20]. In this study the Poisson's ratio value of all resin-composites, was chosen to be 0.3 for the calculation of the moduli. The influence of different Poisson's ratio values, on the calculation of the moduli is presented in Fig. 4. A Poisson's ratio increase by 0.05 caused a decrease of the modulus by about 3–5.5%. An increase of 0.2 (from 0.25 to 0.45) for

the Poisson's ratio would lead to changes of ca. 15% in the moduli values. This is in agreement with previous studies reported that an error in the elastic modulus associated with varying the Poisson's ratio from 0.2 to 0.4 for an isotropic material is at 10% [21, 22].

Direct comparisons of Young's modulus values, obtained from different testing methodologies would not be entirely suitable if the special conditions of each experiment were not taken into account. Young's modulus values measured for polymers using depth sensing indentation devices were significantly higher than values measured using tensile testing [23, 24]. Nanoindentation is mainly a surface technique and possible sample flaws, like the presence of pores, which may affect the bulk properties of materials as measured with other techniques, are unlikely to affect nanoindentation modulus values. Although there have been recent advances in the use of nanoindentation for testing viscoelastic materials [25, 26], this study has utilised nanoindentation theory based on elastic theory. Further work is needed to determine the viscoelastic indentation properties of these model resin-composites.

Filler volume fraction is recognized as the primary factor for Young's modulus determination. Filler size and shape, for the volume fraction used in this study, were found to be *secondary* fine-tuning factors. Even though the Young's modulus values obtained cannot be considered "absolute", the ranking and the trends observed between materials can be very useful in the development of improved commercial formulations.

5 Conclusions

For the materials tested with constant volume-fraction, the filler size of resin-composites seemed to be mainly a *fine-tuning* factor for the determination of Young's modulus. Larger filler sizes tend to render the material stiffer. Filler shape was also found to affect Young's modulus. Irregular filler shapes result in higher modulus values than resin-composites with spherical fillers.

References

1. H. Ralph Rawls, J.F. Esquivel-Upshaw, in *Phillips' Science of Dental Materials*, ed. by K. Anusavice (Saunders, St. Louis, 2003), p. 399
2. L.H. He, M.V. Swain, Dent. Mater. **23**, 814 (2007)
3. N.J. Lin, P.L. Drzal, S. Lin-Gibson, Dent. Mater. **23**, 1211 (2007)
4. J.L. Drummond, J. Biomed. Mater. Res. B Appl. Biomater. **78**, 27 (2006)
5. G. Willems, J.P. Celis, P. Lambrechts, M. Braem, G. Vanherle, J. Biomed. Mater. Res. **27**, 747 (1993)
6. http://www.ceramics.nist.gov/srd/summary/glss100a.htm. Accessed June 2008
7. http://www.ceramics.nist.gov/srd/summary/glss60a.htm. Accessed June 2008
8. W.C. Oliver, G.M. Pharr, J. Mater. Res. **19**, 3 (2004)
9. J.S. Field, M.V. Swain, J. Mater. Res. **8**, 297 (1993)
10. A.C. Fischer-Cripps, *Nanoindentation* (Springer-Verlag, New York, 2002)
11. J. Mencik, M.V. Swain, J. Mater. Res. **10**, 1491 (1995)
12. M. Suganuma, M.V. Swain, J. Mater. Res. **19**, 3490 (2004)
13. C.A. Schuh, Mater. Today **9**, 32 (2006)
14. D.W. Jones, A.S. Rizkalla, J. Biomed. Mater. Res. **33**, 89 (1996)
15. F. Chabrier, C.H. Lloyd, S.N. Scrimgeour, Dent. Mater. **15**, 33 (1999)
16. S.M. Chung, A.U. Yap, W.K. Koh, K.T. Tsai, C.T. Lim, Biomaterials **25**, 2455 (2004)
17. N. De Jager, P. Pallav, A.J. Feilzer, Dent. Mater. **20**, 457 (2004)
18. K. Masouras, N. Silikas, D.C. Watts, Dent. Mater. **24**, 932 (2008)
19. W.T. Nakayama, D.R. Hall, D.E. Grenoble, J.L. Katz, J. Dent. Res. **53**, 1121 (1974)
20. R.W. Warfield, J.E. Cuevas, F.R. Barnet, Rheol. Acta **9**, 439 (1970)
21. J.Y. Rho, T.Y. Tsui, G.M. Pharr, Biomaterials **18**, 1325 (1997)
22. P.K. Zysset, X.E. Guo, C.E. Hoffler, K.E. Moore, S.A. Goldstein, J. Biomech. **32**, 1005 (1999)
23. M.R. VanLandingham, J.S. Villarrubia, W.F. Guthrie, G.F. Meyers, Macromol. Symp. **167**, 15 (2001)
24. H. Lee, S. Mall, P. He, D.L. Shi, S. Narasimhadevara, Y. Yeo-Heung, V. Shanov, M.J. Schulz, Composites Part B: Eng. **38**, 58 (2007)
25. M.L. Oyen, Philos. Mag. **86**, 5625 (2006)
26. M.L. Oyen, Acta Mater. **55**, 3633 (2007)